Talanta 116 (2013) 870–875

Contents lists available at ScienceDirect

Talanta

journal homepage: www.elsevier.com/locate/talanta

Bovine serum albumin coated $CuInS_2$ quantum dots as a near-infrared fluorescence probe for 2,4,6-trinitrophenol detection

Siyu Liu, Fanping Shi, Lu Chen, Xingguang Su*

Department of Analytical Chemistry, College of Chemistry, Jilin University, Changchun 130012, China

ARTICLE INFO

Article history:
Received 8 April 2013
Received in revised form
20 July 2013
Accepted 27 July 2013
Available online 9 August 2013

Keywords:
$CuInS_2$ QDs
Bovine serum albumin
Fluorescence quenching
2,4,6-Trinitrophenol
Near-infrared fluorescent probe

ABSTRACT

In this paper, a novel near-infrared fluorescence probe for the determination of 2,4,6-trinitrophenol (TNP) was developed based on bovine serum albumin (BSA) coated $CuInS_2$ quantum dot (QD). Water-soluble $CuInS_2$ QDs were directly synthesized in aqueous solution with mercaptopropionic acid (MPA) as stablizers, and it was coated by BSA via an amide link interacting with carboxyl of the MPA-capped $CuInS_2$ QDs. The obtained BSA coated $CuInS_2$ QDs (BSA-$CuInS_2$ QDs) can bind TNP in water via the acid–base pairing interaction between electron-rich amino groups of BSA and electron-deficient nitroaromatic rings, and leading the fluorescence quenching of BSA-$CuInS_2$ QDs. The quenched fluorescence intensity of BSA-$CuInS_2$ QDs was proportional to the concentration of TNP in the concentration ranges from 50 nmol/L to 3.0 μmol/L. The detection limit (LOD) for TNP was 28 nmol/L. The developed fluorescence probe showed a excellent resistant to interference of metal ions such as K^+, Na^+, Zn^{2+}, Cu^{2+}, Hg^{2+}, and Pb^{2+}. The developed biosensor was applied to the determination of TNP in spiked water samples with satisfactory results.

1. Introduction

Nitroaromatic compounds that are highly explosive and environmentally deleterious substances deserve societal concern. They are environmental contaminants associated with anthropogenic activities, such as production and use of dyes, explosives, pesticides, and pharmaceuticals [1,2]. Because nitroaromatic compounds have strong electron-withdrawing groups, they are poorly biodegradable in the environment [3]. 2,4,6-Trinitrophenol (TNP), as the first synthesized explosives in the world with strong explosion ability and low safety coefficient, may extensively exist in the soil and ground water near military and industrial facilities that may lead to skin irritation, anemia, and abnormal liver functions, when people inhale, ingest or touch it [4,5]. Besides, TNP has harmful effects on male fertility and is now regarded as a possible human carcinogen [6]. Therefore, it is very important to develop simple and rapid analytical methods to identify and quantify nitroaromatic compounds.

In the past decades, a number of analytical methods, such as liquid and gas chromatography, surface-enhanced Raman spectroscopy, resonance Rayleigh scattering, enzyme linked immunosorbent assays, and electrochemical analysis, etc. [7–15] have been applied to detect nitroaromatic explosives. However, some drawbacks such as complicated extraction, high cost, long operation time and low anti-interference ability existed in these methods limited their applications.

Fluorescence measurements have attracted more attention owing to its low-cost, operational simplicity, high sensitivity, and real-time detection. A series of fluorescence sensors have been designed for the detection of biological molecules, and environmental contaminants, etc. [16–24].

Some research groups introduced the fluorescence measurements into the determination of nitroaromatic compounds in real water samples. So far, most of the reports on the fluorescence determination of nitroaromatic compounds were based on some special fluorescence polymers [25–33]. Trogler et al. reported the fluorescence quenching phenomenon of copolymers containing tetraphenylsilole or tetraphenylgermole with Si–Si, Ge–Ge, and Si–Ge backbones induced by nitroaromatic compounds [26]. Patil and coworkers developed a novel fluoranthene based fluorescent chemosensor for the detection of TNP. In the detection process, static fluorescence quenching was the dominant by intercalative π–π interaction between fluoranthene and nitroaromatics [32].

In comparison with organic dyes and fluorescent proteins, QDs are promising fluorescence material for biosensors that show unique advantages such as high emission quantum yields, narrow and symmetric emission peaks with a broad range of excitation wavelengths, and good chemical and optical stabilities [34–38]. Simonet et al. reported the first observation of selective and specific recognition of chiral L-cysteine (L-cys)- or D-cysteine (D-cys)-capped CdSe/ZnS QDs

* Corresponding author. Tel.: +86 431 85168352.
E-mail address: suxg@jlu.edu.cn (X. Su).

0039-9140/$ - see front matter © 2013 Elsevier B.V. All rights reserved.
http://dx.doi.org/10.1016/j.talanta.2013.07.073

with carnitine enantiomers in aqueous solution [34]. Kim et al. demonstrated inhibition assay of avidin concentration based on fluorescence resonance energy transfer (FRET) between QDs and gold nanoparticles [35]. Most of traditional QDs were nanomaterials with cadmium, and yet the leaks of cadmium from the QDs were toxic to biological systems and eventually caused serious environmental problems. Recently, a novel kind of I–III–VI $CuInS_2$ QDs that does not contain any toxic class A elements (Cd, Pb, and Hg) or class B elements (Se and As) just came into view [39–41]. Based on this consideration, we have previously presented a one-pot synthesis of water-soluble $CuInS_2$ QDs capped with mercaptopropionic acid (MPA) [42].

In this paper, bovine serum albumin (BSA) was covalently linked to the MPA-capped $CuInS_2$ QDs. The obtained BSA coated $CuInS_2$ QDs (BSA-$CuInS_2$ QDs) could effectively bind TNP via the acid–base pairing interaction between electron-rich amino groups of BSA and electron-deficient nitroaromatic rings, that might lead to the fluorescence changes of BSA-$CuInS_2$ QDs. Thus, we developed a novel fluorescence probe for rapid and highly sensitive detection of explosive TNP molecules.

2. Experiment

2.1. Apparatus

The fluorescence spectra were obtained by using a Shimadzu RF-5301 PC spectrofluorophotometer equipped with a xenon lamp using right-angle geometry. UV–vis absorption spectra were obtained by a Varian GBC Cintra 10e UV–vis spectrometer. In both experiments, a 1 cm path-length quartz cuvette was used. FT-IR spectra were recorded with a Bruker IFS66V FT-IR spectrometer equipped with a DGTS detector (32 scans). Dynamic Light Scattering spectra (DLS) were obtained by Zetasizer Nano S90.

2.2. Reagents

All reagents were of at least analytical grade. The water used in all experiments had a resistivity higher than 18 MΩ cm^{-1}. Copper (II) chloride dihydrate ($CuCl_2{\bullet}2H_2O$), sodium hydroxide (NaOH), sulfourea ($CS(NH_2)_2$), sodium dehydrogenized phosphate (NaH_2PO_4) and disodium hydrogen phosphate (Na_2HPO_4) were purchased from Shanghai Qingxi Technology Co., Ltd. BSA, indium (III) chloride tetrahydrate ($InCl_3{\bullet}4H_2O$) 1-ethyl-3-[3-dimethylaminopropyl] carbodiimide hydrochloride (EDC), N-hydroxysuccinimide (NHS), phenol, TNP, dinitrotoluene (DNT), 4-nitrophenol(4-NP), and 2-nitrophenol(2-NP) were purchased from Sigma-Aldrich Corporation. The 0.1 mol/L PBS (pH 7.0, 0.1 mol/L NaH_2PO_4–Na_2HPO_4) was used as the medium for detection process.

2.3. Preparation of MPA-capped $CuInS_2$ QDs

MPA-capped $CuInS_2$ QDs were synthesized in aqueous solution, according to our previous report [42]. 0.15 mmol $CuCl_2{\bullet}2H_2O$ and $InCl_3{\bullet}4H_2O$ were dissolved in 10.5 mL distilled water, and then 1.8 mmol MPA was injected into the solution. The pH value of the mixture solution was adjusted to 11.3 by adding 2 mol/L NaOH solution with stirring during this process. After stirring for 10 min, 0.30 mmol $CS(NH_2)_2$ was dissolved in above solution. The previous process was all finished at room temperature, and then the mixture solution was finally transferred into a 15 mL autoclave. Then it was heated and maintained at 150 °C for 21 h and then cooled down to room temperature by a natural process. Ethanol was added to the stock solution to obtain $CuInS_2$ QDs precipitate, and the process was repeated three times. The unreacted residues were removed by the cycled washing. The purified $CuInS_2$ QDs were dissolved in PBS (0.1 mol/L, pH 7.0), and stored in the dark room.

2.4. Preparation of BSA coated $CuInS_2$ QDs

BSA has amino groups available for the conjugation with carboxylic acid group capping $CuInS_2$ QD via amide formation, using the EDC/NHS coupling reaction. The BSA coated $CuInS_2$ QDs (BSA-$CuInS_2$ QDs) were prepared according to previous report [43–45]. A reaction mixture containing 0.12 mmol/L $CuInS_2$ QDs, 2.0 g/L BSA, 5 mmol/L NHS, 0.05 mol/L EDC in pH 7.4 PBS was prepared and kept at room temperature for 4 h, then stored at 4 °C overnight. This allows the unreacted EDC to hydrolyze and lose its activity. The conjugate solution was centrifugated to separate unreacted BSA (the mass of the unreacted BSA was weighed after drying). And then one can dialyze the solution with Spectra/Por 4 Membrane, MWCO 12,000–14,000 to remove the remaining small molecules. The purified BSA-$CuInS_2$ QDs solution was stored in the darkroom. The mass concentration of BSA coated $CuInS_2$ QDs could be calculated (0.6 mg/mL) after the purified BSA-$CuInS_2$ QDs was precipitated by the addition of excess acetonitrile, dried and weighed. And the mass ratio of the BSA to $CuInS_2$ QDs was calculated to be 4.9:1.

2.5. The detection process

The BSA-$CuInS_2$ QDs solution (200 μL, 0.6 mg/mL), 0.1 mol/L PBS buffer (pH 7.0, 1.0 mL), and different amount of TNP or other aromatic compounds (DNT, 4-NP, 2-NP and phenol) were successively added into a 10 mL calibrated test tube. Then, the solution was diluted to the mark with deionized water followed by the thoroughly shaking and equilibrated for 2 min until the solution was fully mixed. The fluorescence spectra were recorded from 600 nm to 850 nm, and the sampling interval was 1.0 nm. The slit widths of excitation and emission were both 10 nm. The fluorescence (FL) intensity of the maximum emission peak was used for the quantitative analysis of the target molecules.

3. Results and discussions

3.1. Spectral characterization of BSA-$CuInS_2$ QDs

As well-known that, the fluorescence properties of QDs had a close connection to the composition of surface capped layers. Recently, many fluorescence probes have been proposed to recognize molecules and ions by employing some special receptors or ligands to functionalize the original QDs [34,36,43]. In this work we selected BSA to modify the MPA-capped $CuInS_2$ QDs. The fluorescence emission and UV–vis absorption spectra of MPA-capped $CuInS_2$ QDs and BSA-$CuInS_2$ QDs are shown in Fig. 1A. It could be seen that the fluorescence emission peak of MPA-capped $CuInS_2$ QDs around 660 nm was narrow and symmetrical, and the UV–vis absorption peak was around 570 nm, which were consistent with our previous report [42]. After the BSA was connected to $CuInS_2$ QDs, the surface capped layer of the $CuInS_2$ QDs was changed from MPA with negatively charged to BSA that existed amounts of amino groups, and the formed new coated layer increased the size of $CuInS_2$ QDs. As a result, the fluorescence emission peak of the BSA-$CuInS_2$ QDs exhibited a significant red shift to 680 nm.

Fig. S1 shows the FT-IR spectra of the MPA-capped $CuInS_2$ QDs (curve *a*) and BSA-$CuInS_2$ QDs (curve *b*). As shown in the curve *a* in Fig. S1, the majority of MPA functional groups could be clearly found through the C=O stretching peak (1730 cm^{-1}), and C–H stretching mode (2850 cm^{-1}, 2920 cm^{-1}, 2960 cm^{-1}). The characteristic peak

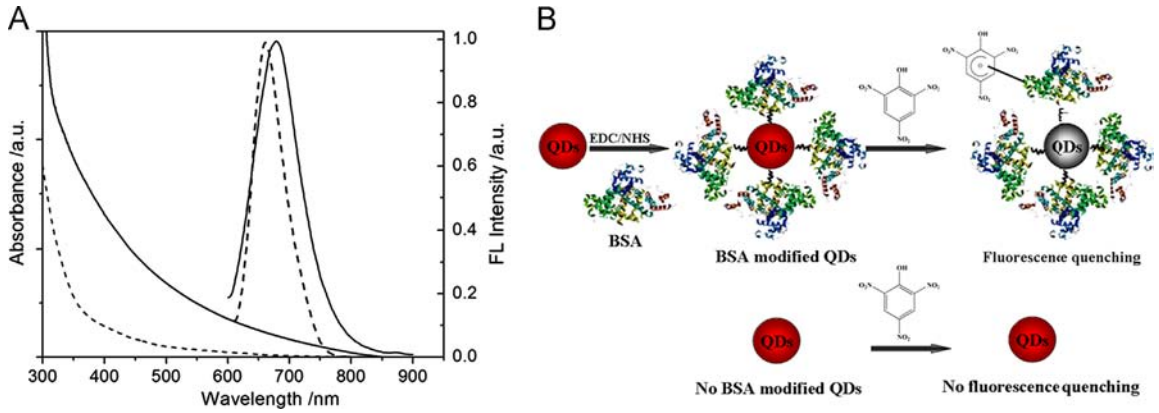

Fig. 1. (A) The UV–vis absorption and fluorescence emission spectra of MPA-capped $CuInS_2$ QDs (dashed line) and BSA-$CuInS_2$ QDs (solid line). (B) The schematic illustration of the synthetic process of BSA-$CuInS_2$ QDs and the TNP detection.

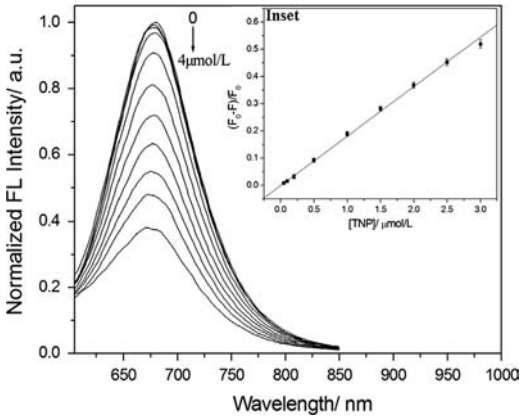

Fig. 2. The fluorescence spectra of BSA-$CuInS_2$ QDs upon the addition of different concentrations of TNP in the range from 0 to 4.0 μmol/L (0, 0.05, 0.10, 0.2, 0.5, 1.0, 1.5, 2.0, 2.5, 3.0, and 4.0 μmol/L). Inset: plot of fluorescence quenching ratios $(F_0-F)/F_0$ of BSA-$CuInS_2$ QDs at 680 nm versus the concentration of TNP. PBS: 10 mmol/L phosphate buffer solution (pH 7.0) at room temperature.

of S–H did not appear within 2550–2680 cm^{-1}, which might be caused by the covalent bonds between thiols and metal. As shown in the curve *b* in Fig. S1, the amide I band (1660 cm^{-1}) and amide II (1540 cm^{-1}) band for –CONH group appeared, which was due to the conjugation of BSA to the MPA capped $CuInS_2$ QDs. In order to prove the presence of BSA after the conjugation, UV–vis absorption spectra (230–500 nm), the fluorescence emission spectra (300–500 nm) and the dynamic light scattering (DLS) of the BSA-$CuInS_2$ QDs were performed. As shown in Fig. S2A, the typical UV–vis absorption peak around 260 nm and fluorescence emission peak around 345 nm (excitation at 280 nm) belonging to BSA were observed in the BSA-$CuInS_2$ QDs, and not observed in the original MPA-capped $CuInS_2$ QDs. As shown in Fig. S2B, the increase of the particle sizes after the conjunction could be observed, which was due to the new capped BSA layers.

3.2. The interactions between TNP and BSA-$CuInS_2$ QDs

As shown in Fig. 1B, the developed BSA-$CuInS_2$ QDs could bind TNP molecule. In this work, the interaction between TNP and BSA-$CuInS_2$ QDs was systematically discussed based on the fluorescence changes of BSA-$CuInS_2$ QDs. Fig. 2 shows the evolution of fluorescence spectra of BSA-$CuInS_2$ QDs with increasing TNP concentration. It could be seen that the fluorescence intensity (FL) of BSA-$CuInS_2$ QDs obviously decreased with TNP concentration increasing from 0 to 4.0 μmol/L. Furthermore, inset in Fig. 2 shows that there was a good linear relationship between the fluorescence quenching ratios $(F_0-F)/F_0$ (F_0 and F are the fluorescence intensity of BSA-$CuInS_2$ QDs without or with TNP) of BSA-$CuInS_2$ QDs and the TNP concentration in the range from 50 nmol/L to 3.0 μmol/L. The regression equation is

$$\frac{F_0-F}{F_0} = 0.0028 + 0.1777\,[\mathrm{TNP}],\quad \mu mol/L \tag{1}$$

The corresponding regression coefficient is 0.999, and the detection limit for TNP was 28 nmol/L, calculated following the 3σ IUPAC criteria. The standard deviation for nine replicate measurements of 0.2 μmol/L TNP is 2.3%.

The organic amino ligands modified nanocrystals utilized as the receptors of nitroaromatic compounds have been mentioned in some previous reports [46–48]. The electron transfer from amino groups to aromatic rings leads to the formation of a Meisenheimer complex between nitroaromatic and the amine group [49–54]. In this study, TNP is a typically electron-deficient compound due to the strong electron-withdrawing effect of the three nitro groups. As shown in Fig. 1B, the BSA-coated $CuInS_2$ QDs with high content of electron-rich amino groups could effectively bond to TNP by the acid–base pairing interaction, and the charge transfer complexing interaction would lead to the fluorescence quenching of BSA-$CuInS_2$ QDs.

As shown in Fig. S3A, we systematically investigated the influence of pH value on the fluorescence intensity of BSA-$CuInS_2$ QDs and BSA-$CuInS_2$ QDs quenched by TNP. It can be seen that when the pH value changed from 6.6 to 9.0, the FL intensity of BSA-$CuInS_2$ QDs solution gradually decreased and the FL intensity of BSA-$CuInS_2$ QDs with TNP solution nearly remained the same. At pH 7.0, the fluorescence quenching ratio $(F_0-F)/F_0$ (F_0 and F are the fluorescence intensity of BSA-$CuInS_2$ QDs without or with TNP) gave the best result for the determination of TNP. Fig. S3B shows the temporal evolution of the fluorescence intensity of BSA-$CuInS_2$ QDs after the addition of 2.5 μmol/L TNP. It could be seen that the fluorescence intensity of BSA-$CuInS_2$ QDs rapidly decreased after the addition of TNP, and reached equilibrium, in 2 min. Therefore, pH 7.0 and reaction time of 2 min were the suitable conditions for the detection process.

3.3. The interactions between DNT, 4-NP or 2-NP and BSA-$CuInS_2$ QDs

As indicated earlier, the electron-withdrawing effect of nitro group played a key role in the interaction between the nitroaromatic TNP and BSA-$CuInS_2$ QDs. In this study, we further investigated the interactions of other nitroaromatic DNT, 4-NP or 2-NP and BSA-$CuInS_2$ QDs. Fig. S3B shows the temporal evolution of fluorescence intensity of BSA-$CuInS_2$ QDs in the presence of

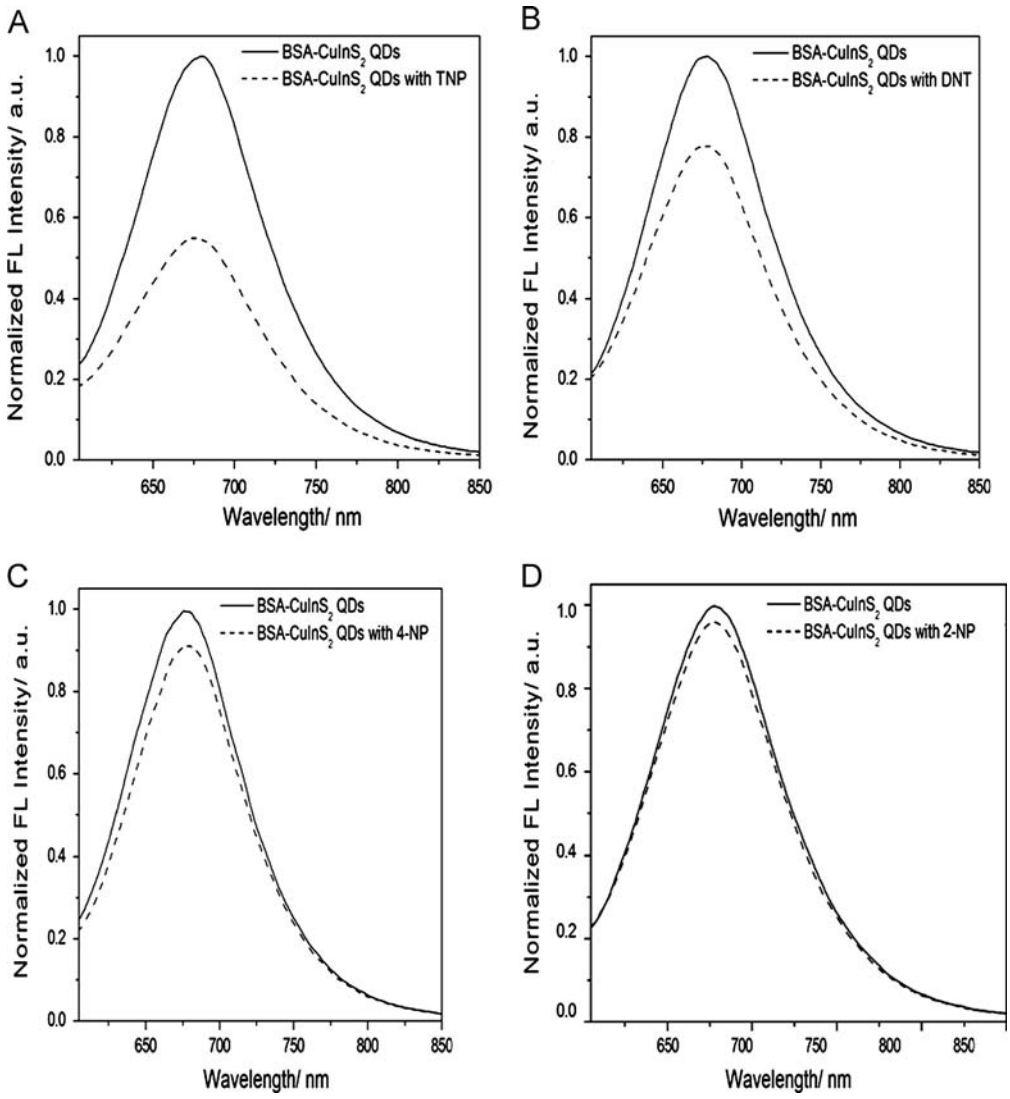

Fig. 3. The fluorescence spectra of BSA-$CuInS_2$ QDs without or with 2.5 μmol/L: (A) TNP; (B) DNT; (C) 4-NP; or (D) 2-NP PBS: 10 mmol/L phosphate buffer solution (pH 7.0) at room temperature.

2.5 μmol/L DNT, 4-NP, 2-NP or phenol respectively. The results demonstrated that the fluorescence intensity of BSA-$CuInS_2$ QDs decreased to some extend after the addition of 2.5 μmol/L DNT, 4-NP or 2-NP, and remained nearly constant in 2 min. The phenol that had no electrophilic nitro groups could not induce the fluorescence quenching of the BSA-$CuInS_2$ QDs. As shown in Figs. 3 and 4A, we compared the fluorescence quenching of BSA-$CuInS_2$ QDs response to TNP, DNT, 4-NP and 2-NP. The results demonstrated that the fluorescence quenching ability of the four nitroaromatic followed the order TNP > DNT > 4-NP > 2-NP, that was consistent with the numbers of nitro groups in the corresponding aromatic ring. Fig. 4B shows the FL intensity of MPA-capped $CuInS_2$ QDs in the presence of different concentration of TNP, DNT, 4-NP or 2-NP. It could be seen that the nitroaromatic TNP, DNT, 4-NP or 2-NP cannot induce obviously fluorescence quenching of MPA capped $CuInS_2$ QDs under the same condition. Therefore, the BSA coating layer of $CuInS_2$ QDs was necessary for the detection process, and it was further confirmed that the fluorescence quenching of BSA-$CuInS_2$ QDs induced by nitroaromatic compounds was due to the acid–base pairing interaction between electron-rich amino groups of BSA and electron-deficient nitroaromatic rings.

3.4. Interference study

In this study, we discussed the effect of a series of foreign metal ions and organics on the fluorescence of BSA-$CuInS_2$ QDs. From Fig. 5, it could be seen that the fluorescence intensity of BSA-$CuInS_2$ QDs system showed the high tolerance concentrations to most common metal ions and organics in water samples. The fluorescence of BSA-$CuInS_2$ QDs remained almost the same even in the presence of 10 μmol/L heavy metal ions such as Cu^{2+}, Hg^{2+}, Ag^{+} or Pb^{2+}. These results indicated that the conjugated BSA layers prevented these metal ions being adsorbed on the surface of $CuInS_2$ QDs. And other common organics such as phenol, benzoic acid, pyridine, etc. also could not induce the fluorescence quenching of BSA-$CuInS_2$ QDs under the same conditions. Therefore, this method has high selectivity and excellent resistance to interference.

Up to now, considerable efforts have been devoted to the development of fluorescence detection for nitroaromatic. For examples, the functionalized fluorescence polymers that usually contain certain amount of aromatic structures have been extensively reported to probe nitroaromatic via π–π electronic attraction [25–33]. However, the complex and expensive polymer synthesis, and the poor water solubility of the fluorescence polymer restricted its application in the

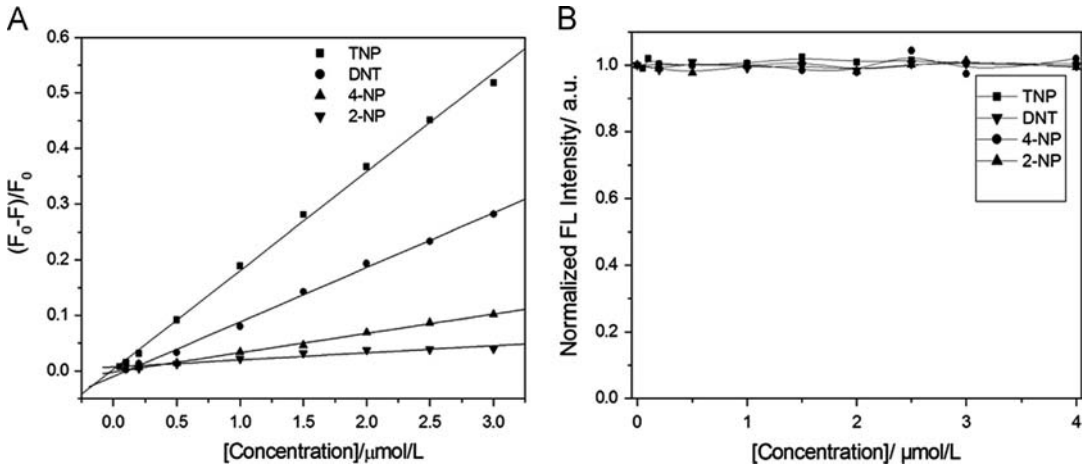

Fig. 4. (A) Plot of fluorescence quenching ratios $(F_0-F)/F_0$ of BSA-$CuInS_2$ QDs at 680 nm versus the concentration of TNP, DNT, 4-NP and 2-NP. (B) Fluorescence intensity of MPA-capped $CuInS_2$ QDs with the increasing concentration of TNP, DNT, 4-NP or 2-NP. PBS: 10 mmol/L phosphate buffer solution (pH 7.0) at room temperature.

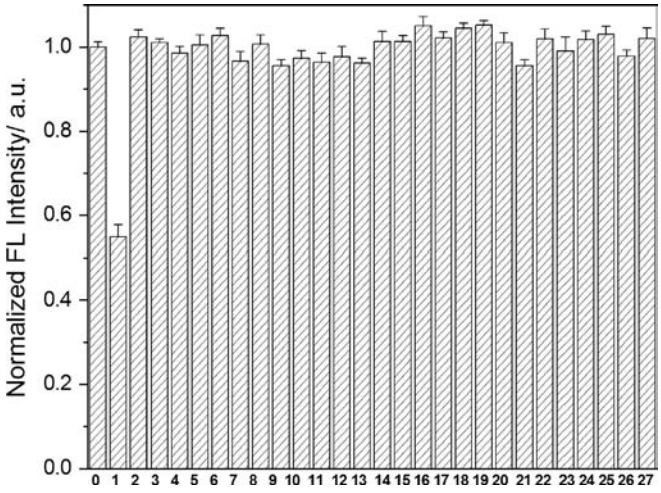

Fig. 5. (0) The fluorescence intensity of BSA-$CuInS_2$ QDs. (1) The fluorescence intensity of BSA-$CuInS_2$ QDs with 2.5 μmol/L TNP. The fluorescence intensity of BSA-$CuInS_2$ QDs with 10 μmol/L. (2) K^+, (3) Ca^{2+}, (4) Na^+, (5) Mg^{2+}, (6) Ba^{2+}, (7) Fe^{3+}, (8) Zn^{2+}, (9) Cu^{2+}, (10) Hg^{2+}, (11) Ag^+, (12) Pb^{2+}, (13) Cd^{2+}, (14) sodium citrate, (15) tartaric acid, (16) glucose, (17) catechol, (18) resorcinol, (19) hydroquinone, (20) benzoic acid, (21) 8-hydroxylquinoline, (22) phenol, (23) ethylene diamine tetra-acetic acid, (24) dimethyl formamide, (25) acetonitrile, (26) pyridine, and (27) furan. PBS: 10 mmol/L phosphate buffer solution (pH 7.0).

Table 1
Determination of TNP in real water samples according to Eq. (1).

Samples	Added (μmol/L)	Found (μmol/L)	Recovery (%)	RSD ($n=3$) (%)
Tap water	0.2	0.18	90	3.5
	1	1.02	102	2.7
Spring water	0.2	0.19	95	2.6
	1	1.05	105	2.3
Chemical plant wastewater	0.2	0.22	110	3.8
	1	1.02	102	3.6

detection of nitroaromatics compounds in water samples. Recently, some functionalized nanoparticles such as L-cysteine capped Mn-doped ZnSe QDs and dendrimer PAMAM capped CdSe QDs, etc. were successfully applied to detect nitroaromatic in water samples [49–56]. However, the fluorescence of these functionalized nanoparticles was easily interfered by some foreign metal ions such as Cu^{2+}, Hg^{2+} and Pb^{2+}, etc. We proposed a water-soluble fluorescence probe BSA-$CuInS_2$ QDs to effectively detect nitroaromatic TNP with high tolerance concentrations to the interference of heavy metal ions. Compared with the previous reports about fluorescence detection for TNP, such as the copolymers containing tetraphenylsilole or tetraphenylgermole as the fluorescence probe for TNP with the dynamic range of 10–100 μmol/L [26], the fluoranthene based fluorescence sensor for the detection of the TNP with the dynamic range of 0.5–10 μmol/L [32], and the paper sensor for TNP-selective detection with the dynamic range of 0.05–7.0 mg/L and the limit detection of 32.3 mg/L [56], our method had the similar detection limit and dynamic range.

3.5. Analytical applications

To test the applicability of the proposed methods, it was applied to determine TNP in tap water, spring water and chemical plant wastewater samples. The water samples were filtered several times through qualitative filter paper. The pH was adjusted to 7.0 using NaOH solution before analysis. The results showed that TNP was not detected in these real samples, so the samples were spiked with standard TNP solution. The averages of three replicate determination results are presented in Table 1. The accuracy of the proposed method was evaluated by determining the average recovery of TNP in real samples. From Table 1, it can be seen that the RSD was lower than 3.8%, and the average recoveries of TNP in the real samples was in the range of 90–110%.

4. Conclusion

In summary, we have demonstrated that the BSA coated $CuInS_2$ QDs could be utilized as a near-infrared fluorescence probe for the detection of TNP. The fluorescence of BSA-$CuInS_2$ QDs was quenched by TNP via the acid–base pairing interaction between electron-rich amino groups of BSA and electron-deficient nitroaromatic rings. Moreover, obvious difference in quenching efficiency was observed for different types of nitroaromatic compounds (TNP, DNT, 4-NP and 2-NP), which is dependent on their electron-accepting ability. The proposed method was simple, convenient and had more resistant to the interference of heavy metal ions and other organics.

Acknowledgments

This work was financially supported by the National Natural Science Foundation of China (Nos. 20875036, 21075050) and the Science and Technology Development Project of Jilin Province, China (No. 20110334).

Appendix A. Supplementary material

Supplementary data associated with this article can be found in the online version at http://dx.doi.org/10.1016/j.talanta.2013.07.073.

References

[1] F.D. Marvin-Sikkema, J.A.M. Bont, Appl. Microbiol. Biotechnol. 42 (1994) 499–507.
[2] P.Z. Lang, X.F. Ma, G.H. Lu, Y. Wang, Y. Bian, Chemosphere 32 (1996) 1547–1552.
[3] N. Fahrenfeld, J. Zoeckler, M.A. Widdowson, A. Pruden, Biodegradation 24 (2013) 179–190.
[4] J.I. Steinfeld, J. Wormhoudt, Annu. Rev. Phys. Chem. 49 (1998) 203–232.
[5] J.V. Goodpaster, V.L. McGuffin, Anal. Chem. 73 (2001) 2004–2011.
[6] M.T.D. Cronin, B.W. Gregory, T.W. Schultz, Chem. Res. Toxicol. 11 (1998) 902–908.
[7] M. Krausa, K.J. Schorb, Electroanal. Chem. 461 (1999) 10–13.
[8] J. Wang, S.B. Hocevar, B. Ogorevc, Electrochem. Commun. 6 (2004) 176–179.
[9] J. Wang, R.K. Bhada, J. Lu, D. MacDonald, Anal. Chim. Acta 361 (1998) 85–91.
[10] W.S. Zou, D. Sheng, X. Ge, J.Q. Qiao, H.Z. Lian., Anal. Chem. 83 (2011) 30–37.
[11] S.S.R. Dasary, A.K. Singh, D. Senapati, H. Yu, P.C. Ray, J. Am. Chem. Soc. 131 (2009) 13806–13812.
[12] P. Jlicher, E. Mussenbrock, R. Renneberg, K. Cammann, Anal. Chim. Acta 315 (1995) 279–287.
[13] T.L. Pittman, B. Thomson, W. Miao, Anal. Chim. Acta 632 (2009) 197–202.
[14] K.E. Sapsford, P.T. Charles, J.C.H. Patterson, F.S. Ligler, Anal. Chem. 74 (2002) 1061–1068.
[15] X. Chen, X.Y. Cheng, J.J. Gooding, Anal. Chem. 84 (2012) 8557–8563.
[16] B. Tang, Y.L. Xing, P. Li, N. Zhang, F.B. Yu, G.W. Yang, J. Am. Chem. Soc. 129 (2007) 11666–11667.
[17] W.T. Wu, T. Zhou, A. Berliner, P. Banerjee, S.Q. Zhou., Angew. Chem. Int. Ed. 49 (2010) 1–6.
[18] J.F. Liu, C.Y. Bao, X.H. Zhong, C.C. Zhao, L.Y. Zhu, Chem. Commun. 46 (2010) 2971–2973.
[19] Y. Zhang, Y. Li, X.P. Yan, Anal. Chem. 81 (2009) 5001–5007.
[20] S. Banerjee, S. Kar, J. Manuel Perez, S. Santra, J. Phys. Chem. C 113 (2009) 9659–9663.
[21] L. Shang, S. Dong, Biosensors Bioelectron. 24 (2009) 1569–1573.
[22] Y.F. Chen, Z. Rosenzweig, Anal. Chem. 74 (2002) 5132–5138.
[23] Q. Ma, E. Ha, F.P. Yang, X.G. Su, Anal. Chim. Acta 701 (2011) 60–65.
[24] Y. Gao, H. Huang, J.J. Hu, S.M. Shah, X.G. Su, Talanta 85 (2011) 1075–1080.
[25] J.C. Sanchez, A.G. DiPasquale, A.L. Rheingold, W.C. Trogler, Chem. Mater. 19 (2007) 6459–6470.
[26] H. Sohn, M.J. Sailor, D. Magde, W.C. Trogler, J. Am. Chem. Soc. 125 (2003) 3821–3830.
[27] Y.H. Lee, H.G. Liu, J.Y. Lee, S.H. Kim, S.K. Kim, J.L. Sessler, Y. Kim, J.S. Kim, Chem. —A Eur. J. 16 (2010) 5895–5901.
[28] Sarah J. Toal, D. Magde, W.C. Trogler, Chem. Commun. 43 (2005) 5465–5467.
[29] N. Niamnont, N. Kimpitak, K. Wongravee, P. Rashatasakhon, K.K. Baldridge, J.S. Siegel, M. Sukwattanasinitt, Chem. Commun. 49 (2013) 780–782.
[30] Y.Y. Long, H.B. Chen, H.M. Wang, Z. Peng, Y.F. Yang, G.Q. Zhang, N. Li, F. Liu, J. Pei, Anal. Chim. Acta 744 (2012) 82–91.
[31] S.J. Chen, Q.Y. Zhang, J.P. Zhang, J.W. Gu, L. Zhang, Sensors Actuators B 149 (2010) 155–160.
[32] N. Venkatramaiah, S. Kumar, S. Patil, Chem. Commun. 48 (2012) 5007–5009.
[33] D.A. Olley, E.J. Wren, G. Vamvounis, M.J. Fernee, X. Wang, P.L. Burn, P. Meredith, P.E. Shaw, Chem. Mater. 23 (2011) 789–794.
[34] C.C. Carrión, S. Cárdenas, B.M. Simonet, M. Valcárcel, Anal. Chem. 81 (2009) 4730–4733.
[35] E. Oh, M.Y. Hong, D. Lee, S.H. Nam, H.C. Yoon, H.S. Kim, J. Am. Chem. Soc. 127 (2005) 3270–3271.
[36] E.R. Goldman, I.L. Medintz, J.L. Whitley, A. Hayhurst, A.R. Clapp, H.T. Uyeda, J.R. Deschamps, M.E. Lassman, H. Mattoussi, J. Am. Chem. Soc. 127 (2005) 6744–6751.
[37] H.F. Dong, W.C. Gao, F. Yan, H.X. Ji, H.X. Ju, Anal. Chem. 82 (2010) 5511–5517.
[38] R.T. Freeman, L. Bahshi, T. Finder, R. Gill, I. Willner, Chem. Commun. 7 (2009) 764–766.
[39] S.L. Castro, S.G. Bailey, R.P. Raffaelle, K.K. Banger, A.F. Hepp, J. Phys. Chem. B 108 (2004) 12429–12435.
[40] H. Nakamura, W. Kato, M. Uehara, K. Nose, T. Omata, S.O.Y. Matsuo, M. Miyazaki, H. Maeda, Chem. Mater. 18 (2006) 3330–3335.
[41] R.G. Xie, M. Rutherford, X.G. Peng, J. Am. Chem. Soc. 131 (2009) 5691–5697.
[42] S.Y. Liu, H. Zhang, Y. Qiao, X.G. Su, RSC Adv. 2 (2012) 819–825.
[43] S.Q. Ge, C.C. Zhang, Y.N. Zhu, J.H. Yu, S.S. Zhang, Analyst 135 (2010) 111–115.
[44] J.M. Liu, L.P. Lin, X.X. Wang, S.Q. Lin, W.L. Cai, L.H. Zhang, Z.Y. Zheng, Analyst 137 (2012) 2637–2642.
[45] S.P. Wang, N. Mamedova, N.A. Kotov, W. Chen, J. Studer, Nano Lett. 2 (2002) 817–822.
[46] D.M. Gao, Z.P. Zhang, M.H. Wu, C.G. Xie, G.J. Guan, D.P. Wang, J. Am. Chem. Soc. 129 (2007) 7859–7866.
[47] C.G. Xie, Z.P. Zhang, D.P. Wang, G.J. Guan, D.M. Gao, J.H. Liu, Anal. Chem. 78 (2006) 8339–8346.
[48] G.J. Guan, Z.P. Zhang, Z.Y. Wang, B.H. Liu, D.M. Gao, C.G. Xie, Adv. Mater. 19 (2007) 2370–2374.
[49] W.S. Zou, J.Q. Qiao, X. Hu, X. Ge, H.Z. Lian, Anal. Chim. Acta 708 (2011) 134–140.
[50] R.Y. Tu, B.H. Liu, Z.Y Wang, D.M. Gao, F. Wang, Q.L. Fang, Z.P. Zhang, Anal. Chem. 80 (2008) 3458–3465.
[51] D.M. Gao, Z.Y. Wang, B.H. Liu, L. Ni, M.H. Wu, Z.P. Zhang, Anal. Chem. 80 (2008) 8545–8553.
[52] Y.F. Chen, Z. Chen, Y.J. He, H.L. Lin, P.T. Sheng, C.B. Liu, S.L. Luo, Q.Y. Cai, Nanotechnology 21 (2010) 125502.
[53] M. Algarra, B.B. Campos, M.S. Miranda, C.G. Esteves da Silva Joaquim, Talanta 83 (2011) 1335–1340.
[54] Y.Q. Wang, W.S. Zou, Talanta 85 (2011) 469–475.
[55] R. Freeman, T. Finder, L. Bahshi, R. Gill, I. Willner, Adv. Mater. 24 (2012) 6416–6421.
[56] Y.X. Ma, H. Li, S. Peng, L.Y. Wang, Anal. Chem. 84 (2012) 8415–8421.